IOPscience iopscience.iop.org

Home Search Collections Journals About Contact us My IOPscience

Radiation-enhanced diffusion of Ag produced by Ar implantation into Ag-doped glass

This article has been downloaded from IOPscience. Please scroll down to see the full text article.

1989 J. Phys.: Condens. Matter 1 5045

(http://iopscience.iop.org/0953-8984/1/31/004)

View the table of contents for this issue, or go to the journal homepage for more

Download details:
IP Address: 171.66.16.93
The article was downloaded on 10/05/2010 at 18:32

Please note that terms and conditions apply.

J. Phys.: Condens. Matter **1** (1989) 5045–5050. Printed in the UK

Radiation-enhanced diffusion of Ag produced by Ar implantation into Ag-doped glass

A K Sbouh, D-E Arafah and Y Al-Ramadin
Physics Department, University of Jordan, Amman, Jordan

Received 1 November 1988, in final form 4 January 1989

Abstract. The Rutherford back-scattering spectrometry (RBS) technique has been used to investigate radiation-enhanced diffusion (RED) of silver in Ag-doped soda-lime glass bombarded with 9×10^{15} ions cm^{-2} $^{40}Ar^+$ implanted at 280 keV. The depth distribution of Ar impurities was measured. Range and straggling data for 280 keV Ar impurities were determined. Good agreement to within experimental uncertainties is obtained when a comparison with theoretical estimates and other work is made. The RBS energy spectra reveal a distinct peak near 1.5, the projected range of Ar due to Ag migrating towards larger depths; this peak is accounted for in terms of inter-diffusion processes resulting from the RED mechanism. Depletion in the oxygen signal was also noted and interpreted as being due to preferential sputtering of oxygen from the surface.

1. Introduction

Rutherford back-scattering spectrometry (RBS) has proven to be a powerful tool in materials analysis [1, 2]. Obtaining information about impurities, their stability and their depth distribution in the near-surface regions of solids constitutes a major step in characterising the properties of materials under investigation [3]. Upon irradiation, insulating materials exhibit many interesting features and reveal potential applications [4–7].

The conventional method of ion implantation induces controlled changes in the surface and near-surface properties of solids. Modifications of the properties of materials are also possible if the impurities are introduced by thermal or electric-field-enhanced diffusion processes [8–11]. Such induced effects are extensively documented for semiconductors and metals but are rather poorly documented for insulators [12].

Radiation-enhanced diffusion (RED) effects, which appear as a consequence of irradiation, are mostly studied for ion-implanted metals and alloys. In all cases, the implantation causes variations in the defect depth distribution and both experimental [13, 14], and theoretical [15] results explain this phenomenon. Parallel examples of insulators were also observed [16, 17].

The first step in all ion implantation studies is the determination of the ion range and the extent of the radiation damage in the implanted material. In addition, one must consider the stability of impurities and lattice defects. The present work reports on some radiation-enhanced diffusion experiments on silver-doped soda-lime glass after 280 keV argon bombardment.

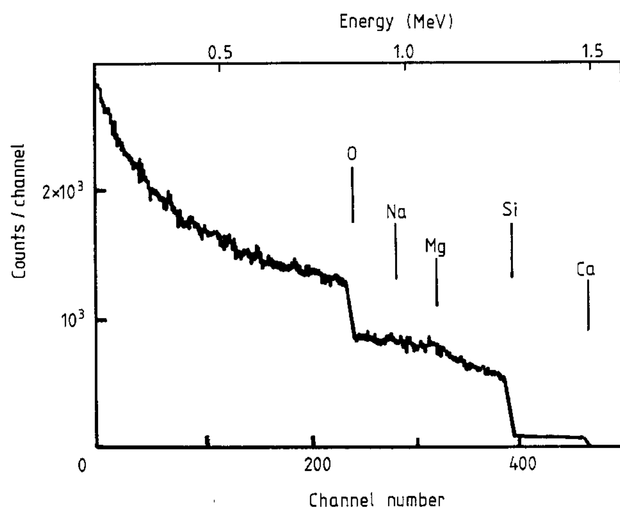

Figure 1. A typical 2 MeV $^{4}He^{+}$ RBS energy spectrum of a soda-lime glass sample. The markers indicate the surface scattering energies from all elements present in the matrix.

2. Experimental details

Soda-lime glass samples of known composition were used in this work. The glass matrix was known to contain the following nominal compositions: 71.8 wt% SiO_2, 15.3 wt% Na_2O, 7.4 wt% CaO, 4.0 wt% MgO and 1.5 wt% other impurities. Silver was introduced into the glass matrix by a thermal ion exchange diffusion process. The diffusion process, doping, which lasted for 30 min, was carried out using one molar concentration of $AgNO_3$ solution. The solution was prepared in a dark room because silver ions are sensitive to light. No electric field was used to enhance the diffusion process and all the experiments were conducted at room temperature. The samples were gently rinsed in a bath of distilled water after removal from the solution and prior to irradiation.

The silver-doped glass samples were implanted with 280 keV $^{40}Ar^{+}$ ions supplied from the University of Jordan Van de Graaff accelerator (JOVAC). The irradiation fluence was kept constant at 9×10^{15} ions cm^{-2}. A relatively low beam flux density of 100 to 150 nA cm^{-2} was used. The beam was directed into the chamber through a beam line of length 4 m. The path to the chamber was equipped with a beam viewer and a pair of tantalum collimators. No beam scanning was used and homogeneity was achieved by defocusing the beam over a 1 cm^2 target area. The energy stabilisation of the beam was a few keV. The typical working pressure during irradiation and analysis was about 10^{-4} Pa and was reached using a turbo-molecular pump. A biasing arrangement was incorporated to suppress secondary-electron emission from the target. All irradiation experiments were carried out at normal incidence and room temperature.

The RBS analysis was performed using 2 MeV $^{4}He^{+}$ ions. The back-scattered particles were collected using silicon surface barrier detector of 16 keV full width at half maximum (FWHM) resolution and a standard RBS geometry [1]. A total angle of scattering of 135° was used. The collected spectra were stored in an IBM-PC/XT microcomputer for further analysis. The Ar-impurity distribution was obtained from figure 2 using a channel-by-channel subtraction procedure after normalising to the same ^{4}He dose. This procedure can be justified by noting that prior to treatment with silver, some changes occur in the oxygen signal, whereas the changes are insignificant in the Ca signal, which mainly overlaps with the Ar impurity profile. The impurity profile distributions are

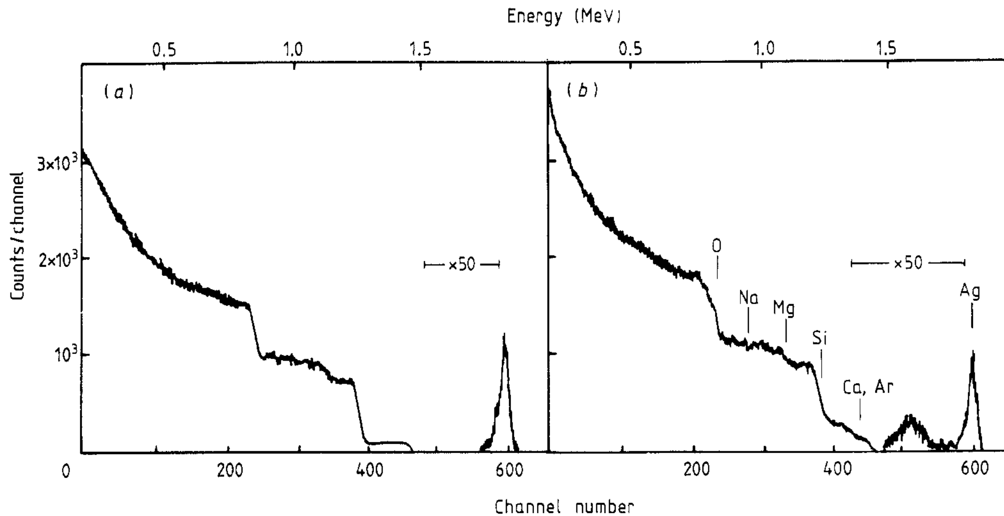

Figure 2. The RBS energy spectrum of 2 MeV $^4He^+$ back-scattered from a glass sample after thermal diffusion in $AgNO_3$ solution for 30 min (*a*), and then implantation with 9×10^{15} ions cm^{-2} $^{40}Ar^+$ at 280 keV (*b*). We suggest that the small peak formed at channel number 505 is due to Ag migration, towards larger depths.

approximately Gaussian. The parameters that describe the distribution were determined by fitting the obtained experimental data to an asymmetrical Gaussian function. The curve-fitting approach adopted was statistical, using variational calculus to minimise the sum of the squares of the fitting coefficients [18]. The parameters obtained represent the maximum or projected range, R_p, the mean range, $\bar{R}$, and the range straggling, ΔR_p, of the impurity distribution. For convenience, these values are given in units of Å (or nm), assuming the layer density to equal the target density, $\rho = 2.21$ g cm^{-3}.

3. Results and discussion

Figure 1 shows the resulting RBS energy spectrum of 2 MeV $^4He^+$ ions incident on glass. The markers indicate the surface scattering energies from all elements constituting the matrix. The RBS energy spectrum of the same sample after a 30-minute doping in $AgNO_3$ solution is presented in figure 2(*a*), and that after 280 keV $^{40}Ar^+$ implantation is shown in figure 2(*b*). Figure 2(*b*) clearly indicates the presence of both Ar and Ag impurities when compared with figure 1. Several points are worth mentioning in relation to figure 2(*b*). First, the Ar impurity signal overlaps with the matrix signal resulting from calcium. The Ar signal was, however, extracted after normalising to the same $^4He^+$ dose, and plotted as shown in figure 3. Second, two distinctly different peaks, at 1.53 and 1.78 MeV, were detected. The smaller peak was absent after the silver diffusion (cf figure 2). Spectra like the ones shown in figures 1 and 2 eliminate the possibility of high-mass tracers being present in the matrix, and hence no signal overlap is expected beyond the Ca signal. We suggest that the presence of the second peak, where it is detected, is due to silver migration, towards larger depths. This is reasonable and may be accounted for in terms of radiation-enhanced diffusion of silver caused by the argon irradiation. The energy

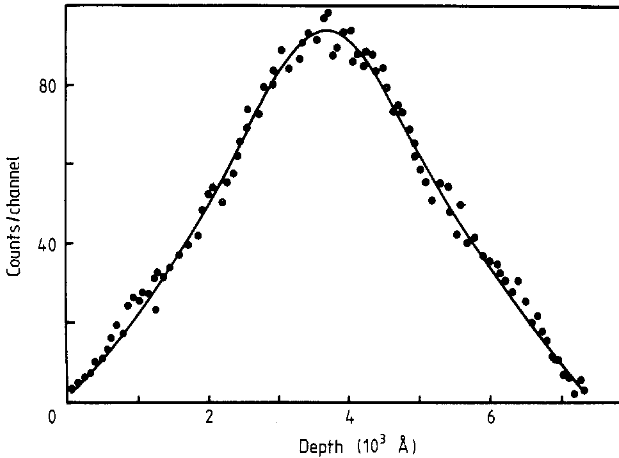

Figure 3. The extracted ^{40}Ar distribution profile plotted as a function of depth (280 keV $^{40}Ar^+ \rightarrow$ glass; dose = 9×10^{15} ions cm^{-2}). The full curve was fitted to the experimental data points.

Table 1. Projected range, R_p, mean range, $\bar{R}$, and range straggling, ΔR_p, data for 280 keV $^{40}Ar^+$ ions implanted into glass, SiO_2 and other materials representing the average mass of the target matrix.

E_0 (keV)	R_p (nm)	$\bar{R}$ (nm)	ΔR_p (nm)	Target	Reference
300	320	360	—	Glass	[21]
280	600	580	330	Neon	[19]
280	370	340	240	Glass	[19]
300	320	360	—	Glass	[21]
280	240	270	150	SiO_2	[25]
300	180	—	120	Si_3N_4	[26]
300	160	—	100	Al_2O_3	[26]
280	360	360	240	Glass	This work
280	370	—	—	Glass	This work, using the analytical formula of Chu

difference between the two peaks is 245 keV (about 550 nm) whereas the projected range, R_p, of Ar is measured to be 360 nm (cf table 1). This implies that the second peak is located at about 1.5 times the value of R_p for argon. It is possible that the second peak may be formed in regions where there is a high concentration of defects (regions near 210 nm [19]), i.e. near the strained layer created by the Ar implantation, but it is more probable that the peak will form near the projected range of the Ar impurity profile. The total depth corresponding to Ar impurities, assuming a Gaussian distribution, is about 720 nm and silver is detected in that layer. It should be mentioned that the damage created by the Ar irradiation, which is mainly nuclear damage, is not only efficient in forcing more silver migration toward regions where the concentration gradient of defects is at its maximum but also extends over the strained layer of depth 1.5 R_p. This may be because during the implantation process a high dislocation density is produced by the radiation damage at depths exceeding 210 nm. This tentative suggestion can be checked if the energy of the beam is increased—one then expects more Ag migration and a smeared distribution to be observable. This was not attempted due to the limits on the

bending powers of both the analysing and switching magnets. Similar observations were made earlier in which a second distribution is formed after Kr implantation into glass [20, 21]. The latter was accounted for as arising from radiation compaction of the glass matrix.

Examining the oxygen signal more closely reveals stepwise changes of the intensity of the signal at channel numbers 219 and 229 (cf figure 2(*b*)). The energy difference corresponds to a depth of oxygen of about 62.5 nm. This oxygen-depleted region is also part of the disturbed layer, which extends to about 720 nm. It should be noted that due to the strong bond between silicon and oxygen, any depletion present would be minimal. Oxygen, however, is the lightest element present in the matrix and is expected to be preferentially sputtered from the surface. The loss of oxygen is due to the radiation damage introduced by the Ar beam and extends to about 17% below the surface. Changes in the surface topography due to Ar bombardment have been previously observed in glass using scanning electron microscopy (SEM) studies [22]. However, changes in the surface topography induced by the implantation process can have a marked influence on the measured depth profile. For example, one expects changes in the surface composition, which produce a reduction in the surface density of the target, due to the preferential sputtering of oxygen. Such an effect gives an RBS calculation that will underestimate the depth of the peak as measured from the surface. This appears to be insignificant in our determination of the argon R_p-values, for excellent agreement, to within experimental uncertainties, is obtained (see later). On the other hand, one expects changes in the Na distribution because the Na ions are the only ions that are mobile during the exchange process [23, 24]. However, due to the well known limitations of the RBS technique, obtaining depth information on Na is difficult using this method. Nevertheless, this work clearly demonstrates changes in the composition of the matrix due to irradiation.

The values of R_p, $\bar{R}$ and ΔR_p obtained from the results of this work are listed in table 1. Values from other work are also included for comparison. The range straggling values represent the FWHM of the distributions. There is reasonable agreement, to within experimental uncertainties, between our values and those obtained from Bayley and Townsend's measurements [21] and the calculations of Ziegler and co-workers [19]. However, our values are higher by about 35% than those calculated by LSS [25]. The discrepancies are mainly due to the stopping power values used by the LSS. Chu and co-workers [26] found an analytical formula for the range of implanted impurities, namely

$$R_p\ (\text{Å}) = (1/\rho)(530/Z)\, E_0\ (\text{keV})$$

where ρ is the density of the target in g cm^{-3}, Z is the atomic number of the incident ions and E_0 is the incident ion energy in keV. Using the above expression, with $Z = 18$ and $E_0 = 280$ keV, one obtains a depth of 3730 Å (or 373 nm), in excellent agreement with the average value of R_p obtained in this work.

The main uncertainties inherent in this work have many sources. These include $\pm 8\%$ uncertainty in the stopping powers [19], and detector and energy straggling resolutions. Signal overlap constitutes another difficulty in our measurements. All the problems were resolved by normalisation and by carrying out deconvolution procedures for the data obtained. The overall uncertainty in this work is about $\pm 10\%$. Finally, the excellent agreement with theory and other work gives further support as regards the reliability of the results obtained.

4. Conclusion

In conclusion, the present experiment gives an example of radiation-enhanced diffusion in insulators favouring impurity motion. This is demonstrated by a second distribution of silver impurities located in the disturbed layer created by Ar implantation being observable. Preferential loss of oxygen, which is the lightest element in the matrix, was also noted, in addition to the Na loss observed by other groups. Range and straggling data have been measured. The excellent agreement with theory and other work confirms that reliable results are obtained.

Acknowledgments

One of us (D-E Arafah) would like to acknowledge Stiftung Volkswagenwerk for financial support.

References

[1] Chu W K, Mayer J W and Nicolet M-A 1978 *Backscattering Spectrometry* (New York: Academic)
[2] Lever R F 1976 *Ion Beam Surface Layer Analysis* vol 2, ed. O Meyer, G Linker and F Kaeppler (New York: Plenum) p 163
[3] Mayer J W, Nicolet M-A and Chu W K 1976 *Material Characterisation Using Ion Beams* ed. J P Thomas and A Cachard (New York: Plenum) p 333
[4] Townsend P D and Valette S 1980 *Optical Effects of Ion Implantation, A Treatise on Materials Science and Technology* vol 19, ed. J K Hirvonen (New York: Academic) ch 11
[5] Arnold G W 1984 *Proc. 2nd Int. Conf. Radiation Effects in Insulators (Albuquerque) 1983* ed. G W Arnold and J A Borders (Amsterdam: North-Holland)
[6] Ketenkamp U, Karge H and Pragner R 1980 *Radiat. Eff.* **48** 31
[7] Arafah D-E, Bangert U, Thiel K and Townsend P D 1983 *Nucl. Instrum. Methods* **209/210** 1105
[8] Gottardi V, Raccanelli A, Della Mea G, Drigo A, Lo Russo S, Mazzoldi P and Kusstatscher P 1976 *Glass Technol.* **17** 1
[9] Lanford W A, Burman C and Ernsberger F 1982 *Bull. Am. Ceram. Soc.* **61** 321
[10] Miotello A and Mazzoldi P 1983 *J. Phys. C: Solid State Phys.* **16** 221
[11] O'Conner D J, Palmer D W, Townsend P D, Morris J, Pitt C W, Neuman Z and Walpite L M 1981 *Nucl. Instrum. Methods* **182/183** 797
[12] Townsend P D 1981 *Nucl. Instrum. Methods* **182/183** 727
[13] Marwick A D, Piller R C and Sivell P M 1979 *J. Nucl. Mater.* **83** 35
[14] Harris D R and Marwick A D 1980 *Phil. Trans. R. Soc.* A **292** 197
[15] Piller R C and Marwick A D 1979 *J. Nucl. Mater.* **83** 42
[16] Bangert U, Arafah D-E, Sassmannhausen U, Thiel K and Townsend P D 1983 *Nucl. Instrum. Methods* **209/210** 1111
[17] Thiel K, Sassmannhausen U, Arafah D-E and Recker K 1984 *Nucl. Instrum. Methods* B **1** 282
[18] Marquardt D W 1963 *J. Soc. Indust. Appl. Math.* **2** 431
[19] Ziegler J F, Biersack J P and Littmark N 1985 *The Stopping and Ranges of Ions in Solids* vol 1, ed. J F Ziegler (New York: Pergamon)
[20] Matzke H J 1966 *Phys. Status Solidi* **18** 285
[21] Bayley A R and Townsend P D 1973 *Optics and Laser Technology* (New York: Academic) p 1079
[22] Chinellato V, Gottardi V, Lo Russo S, Mazzoldi P, Nicoletti F and Polato P 1982 *Radiat. Eff.* **65** 31
[23] Doremus R 1975 *J. Non-Cryst. Solids* **33** 261
[24] Doremus R 1983 *J. Non-Cryst. Solids* **55** 143
[25] Johnson W S and Gibbons J F 1970 *LSS Projected Range Statistics in Semiconductors* (Stanford: University Bookstores)
[26] Chu W K, Crowder B L, Mayer J W and Ziegler J F 1973 *Ion Implantation in Semiconductors and Other Materials* ed. B L Crowder (New York: Plenum) p 225